Ion Distribution Function Evaluation Using Escaping Neutral Atom Kinetic Energy Samples

Pavel R. GONCHAROV, Tetsuo OZAKI, Evgeny A. VESHCHEV and Shigeru SUDO

National Institute for Fusion Science, Toki, Gifu 509-5292, Japan

(Received 16 November 2007 / Accepted 7 March 2008)

A reliable method to evaluate the probability density function of escaping atom kinetic energies is required for analyzing neutral particle diagnostic data used to study the fast ion distribution function in fusion plasmas. In this paper, digital processing of solid state detector signals is proposed as an improvement of the simple histogram approach. Probability density function of kinetic energies of neutral particles escaping from plasma has been derived in a general form, taking into consideration the plasma ion energy distribution, electron capture and loss rates, superposition along the diagnostic sight line, and the magnetic surface geometry. A pseudorandom number generator has been realized to simulate a sample of escaping neutral particle energies for given plasma parameters and experimental conditions. Empirical probability density estimation code has been developed and tested to reconstruct the probability density function from simulated samples assuming Maxwellian ion energy distribution shapes for different temperatures and classical slowing down distributions with different slowing down times. The application of the developed probability density estimation code to the analysis of experimental data obtained by the novel Angular-Resolved Multi-Sightline Neutral Particle Analyzer has been studied to obtain the suprathermal particle distributions. The optimum bandwidth parameter selection algorithm has also been realized.

Keywords: neutral particle analysis, ion distribution, statistical data processing, empirical probability density, kernel bandwidth selection

DOI: 10.1585/pfr.3.S1083

1. Introduction

Measurements of kinetic energy distributions of neutral atoms escaping from magnetically confined plasma in controlled fusion experiments are performed to investigate the ion component distribution function and its evolution due to the application of various plasma heating schemes. The ion distribution function reflects the kinetic effects, the single particle confinement properties depending on the particular magnetic configuration, the finite β effects such as magnetohydrodynamics (MHD) induced fast ion losses, radial electric field effects, etc. The nuclear fusion reaction rate is determined by the ion distribution, and thus, its studies at suprathermal energies near the rate coefficient curve maximum are of primary importance. Advanced neutral particle diagnostics based on solid state detectors with high energy resolution, e.g. [1,2], are used to study the suprathermal ion distribution function. Statistical data processing is required to obtain a smooth normalized energy probability density function (PDF) using random samples of the measured values of particle energies [3].

2. Escaping Neutral Particle Energy Distribution

Without loss of generality, we are considering measurements of fast neutral hydrogen fluxes. The same formalism applies to neutral helium in case of energetic α-particle studies by means of charge exchange diagnostics. The probability density function $f(E)$ for kinetic energies of neutral H^0 particles escaping from the plasma of a magnetic confinement fusion (MCF) device and measured along a line of sight tangent to a magnetic surface $\rho_{\min}$ is given by

$$f(E) = A \exp\left\{\int_{\rho_{\min}}^{1} Q^{-}(\tilde{\rho})\lambda_{\mathrm{mfp}}^{-1}(E,\,\tilde{\rho})\mathrm{d}\tilde{\rho}\right\}\int_{\rho_{\min}}^{1} g\,(E,\rho) \times\left[Q^{+}(\rho)\exp\left\{-\int_{\rho_{\min}}^{\rho} Q^{+}(\tilde{\rho})\lambda_{\mathrm{mfp}}^{-1}(E,\,\tilde{\rho})\mathrm{d}\tilde{\rho}\right\}\right. - \left. Q^{-}(\rho)\exp\left\{-\int_{\rho_{\min}}^{\rho} Q^{-}(\tilde{\rho})\lambda_{\mathrm{mfp}}^{-1}(E,\,\tilde{\rho})\mathrm{d}\tilde{\rho}\right\}\right]\mathrm{d}\rho, \quad (1)$$

where A is the normalization constant calculated so that

$$\int_{0}^{+\infty} f(E)\mathrm{d}E = 1. \quad (2)$$

The local source function for H^0 atoms of energy E within the plasma

$$g(E,\rho) = n_{\mathrm{i}}(\rho) f_{\mathrm{i}}(E,\rho)\sum_{l} n^{(l)}(\rho)\,\langle\sigma\mathrm{v}\rangle^{(l)} \quad (3)$$

author's e-mail: pavel@nifs.ac.jp

is expressed via the local plasma proton distribution $n_i(\rho)f_i(E,\rho)$ and the sum of frequencies of electron capture by protons over all targets for the electron capture process $H^+ \to H^0$. The knowledge of radial profiles of target densities $n^{(l)}(\rho)$ and electron capture rate coefficients $\langle\sigma v\rangle^{(l)}$ is required.

The derivatives $Q^+(\rho) = d\Lambda/d\rho > 0$ and $Q^-(\rho) = d\Lambda/d\rho < 0$ of the sight line distance Λ along the two intervals between $\rho = 1$ and $\rho = \rho_{\min}$ are obtained from the known experiment geometry and the structure of magnetic surfaces $\rho = \text{const}$. Integration in (1) reflects the fact that probabilities for particles that come from different locations are additive. The neutral flux attenuation in the plasma column is multiplicative and takes the form of Poisson exponents, where $\lambda_{\text{mfp}}(E,\ \rho)$ is the local H^0 mean free path with respect to all electron loss reactions $H^0 \to H^+$. From the practical viewpoint, it can be calculated as

$$\lambda_{\text{mfp}}^{-1}(E,\ \rho) = n_e(\rho)\sigma_s(E) \tag{4}$$

using the approximate formula

$$\sigma_s(E,\ \rho) = \frac{\exp\left[S_1(E, n_e, T_e)\right]}{E} \times \left[1 + \frac{1}{n_e}\sum_j n_j Z_j(Z_j - 1) \times S_j(E, n_e, T_e)\right] \tag{5}$$

from [4] for neutral hydrogen stopping cross section in MCF plasma. Radial profiles of electron density n_e and electron temperature T_e are required. n_j and Z_j are impurity densities and charges. The functions $S_1(E, n_e, T_e)$ and $S_j(E, n_e, T_e)$ were derived in [4] for a hydrogen plasma containing He, C, O, and Fe impurities. Alternatively, $\lambda_{\text{mfp}}(E,\ \rho)$ can be calculated for any given plasma composition using the relevant cross section data.

3. Random Energy Samples

Ideally, the passive diagnostic data is an array $(E_1, \ldots, E_N)$ of energies of escaped neutral particles measured along a certain observation direction, and N is the total number of particles collected during a certain time interval. This array is a sample of realizations of the random variable E distributed according to equation (1). Such form of data is achievable with solid state detectors using pulse height analysis (PHA) techniques, while the other analyzers, e.g., $\vec{E} \parallel \vec{B}$ ones, intrinsically form a histogram of the incoming particle energies over a certain number of subintervals called energy channels. Histogramic data representation is often used in solid state detector digital signal processing as well; however, it is possible to collect "raw" data, i.e., pulse height values, directly from a PHA mode analog to digital converter. Technical details may be found in [1, 2].

The formulation of the problem considered here is to obtain an estimate $f^{(*)}(E)$ of the unknown exact probability density function $f(E)$ of neutral particle energies from the experimental data. The sought function preferably should satisfy a specified precision criterion. The obtained PDF estimate is then to be used to reconstruct the ion distribution for further analysis.

Two typical ion energy distribution laws have been used in the numerical simulation of escaped neutral atom energies, namely, (a) Maxwellian distribution with ion temperature T_i

$$f_i(E) = \frac{2}{\sqrt{\pi}}\frac{1}{T_i}\sqrt{\frac{E}{T_i}}\exp(-E/T_i), \tag{6}$$

$$F_i(E) = \frac{2}{\sqrt{\pi}}\gamma\left(\frac{3}{2},\ \frac{E}{T_i}\right), \tag{7}$$

where $\gamma(z, x) = \int_0^x t^{z-1}e^{-t}dt$ is the lower incomplete gamma function; and (b) the classical slowing down distribution for a delta-like fast ion source function

$$S(v - v_0) = \frac{S_0}{4\pi v^2}\frac{\exp\{-(v - v_0)^2/\epsilon^2\}}{\epsilon\sqrt{\pi}}, \tag{8}$$

$$f_i(v) = \frac{S_0}{8\pi}\frac{\tau_s}{v^3 + v_c^3}\left[\text{erf}\left(\frac{v^*(v,t) - v_0}{\epsilon}\right) - \text{erf}\left(\frac{v - v_0}{\epsilon}\right)\right], \tag{9}$$

where the slowing down time

$$\tau_s = \frac{3m_p T_e^{3/2}}{4\sqrt{2\pi}n_e e^4 \Lambda m_e^{1/2}}, \tag{10}$$

the critical velocity

$$v_c^3 = \frac{3\sqrt{2\pi}T_e^{3/2}}{2m_p m_e^{1/2}}, \tag{11}$$

Λ is the Coulomb logarithm, and as shown in [5],

$$v^*(v,t) = \left[\left(v^3 + v_c^3\right)e^{3t/\tau_s} - v_c^3\right]^{1/3}. \tag{12}$$

The ion velocity $v = \sqrt{2E/m_p}$, v_0 is the injection velocity corresponding to the injection energy E_0, the values S_0 and ϵ in (8) determine the source rate and peak width, respectively, and t is the time since the commencement of the fast particle source action.

4. Numerical Experiment

Assuming a predefined theoretical ion energy PDF $f_i(E)$, one can use (1)-(5) to calculate the charge exchange atom energy PDF $f(E)$ and perform a numerical experiment by generating a sample of escaped atom energies for given plasma parameters and experimental conditions. We apply the inverse cumulative distribution function (CDF) approach. First, a sample of N pseudorandom numbers $(u_1, \ldots, u_N)$ uniformly distributed within the (0,1) interval is generated using an algorithm provided in [6]. Then, the energy values are calculated as solutions of the equation

$$F(E_j) = u_j, \tag{13}$$

where

$$F(E) = \int_0^E f(\tilde{E})\mathrm{d}\tilde{E} \tag{14}$$

is the CDF. These simulation results can be supplied as input data for the PDF estimation procedure to test its performance, since the original exact $f(E)$ used in the simulation is known.

Numerical experiments have been performed assuming Angular-Resolved Multi-Sightline (ARMS) Neutral Particle Analyzer (NPA) [2] measurement geometry for one of its lines of sight as depicted in Fig. 1. Large Helical Device (LHD) magnetic surface structure was used, obtained by Variational Moments Equilibrium Code calculation of 3D MHD equilibrium assuming nested flux surfaces [7]. Figure 1 (a) shows effective radius isolines ρ = const., i.e., the magnetic surfaces, in the vertical plane containing the diagnostic sight line. Figure 1 (b) shows ρ values versus the distance Λ along the observation direction and corresponding positive and negative branches of the generalized Abel integral kernel for this sight line and for the assumed MHD equilibrium.

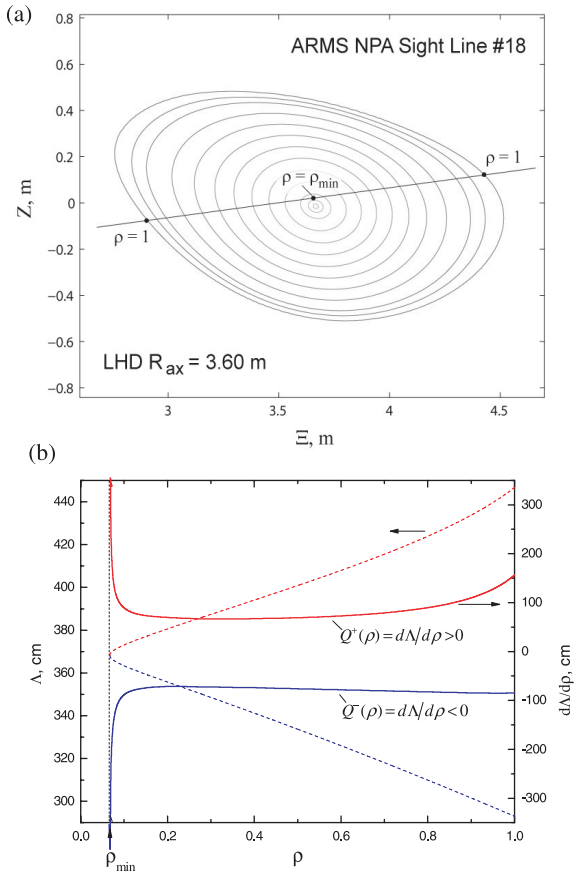

Fig. 1 (a) Cross section of nested LHD magnetic surfaces at R_{ax} = 3.60 m by vertical plane containing ARMS NPA line of sight #18; (b) positive and negative branches of general Abel integral for ARMS NPA sight line #18.

The following functions were used to describe radial profiles of electron density $n_e(\rho)$, electron temperature $T_e(\rho)$, and ion temperature $T_i(\rho)$ in case of Maxwell distribution

$$n_e(\rho) = n_e(0)\,(1-\rho^m)^n\,, \tag{15}$$

$$T_e(\rho) = T_e(0)\,(1-\rho^p)^q\,, \tag{16}$$

$$T_i(\rho) = T_i(0)\,(1-\rho^u)^v\,, \tag{17}$$

with positive superscripts. A simple lower-bound estimate of the background neutral hydrogen density can be obtained from ionization balance as described in [8]

$$\frac{n_0(\rho)}{n_e(\rho)} = \frac{\langle\sigma_{\mathrm{rec}}\mathrm{v}\rangle}{\langle\sigma_{\mathrm{ei}}\mathrm{v}\rangle + \langle\sigma_{\mathrm{ii}}\mathrm{v}\rangle}, \tag{18}$$

with radiative recombination rate $\langle\sigma_{\mathrm{rec}}v\rangle$ given in [9], and electron impact ionization rate $\langle\sigma_{\mathrm{ei}}v\rangle$ and ion impact ionization rate $\langle\sigma_{\mathrm{ii}}v\rangle$ from [10, 11]. A more sophisticated approach to estimate $n_0(\rho)$ requires Monte Carlo modeling analogous to [12] including full 3D tracing of neutral particle trajectories.

Proton-hydrogen charge exchange cross section was taken from [11] to calculate the local source function of H^0 atoms. The attenuation of neutral hydrogen flux was calculated using (5). Figure 2 illustrates the stopping cross section $\sigma_s(E,\rho)$ calculation for two cases, namely, for pure hydrogen plasma with unit effective plasma ion charge Z_{eff} = 1.0 and for Z_{eff} = 1.5, assuming the impurity density ratio to be He:C:O:Fe = 5.00:1.50:0.50:0.05 as suggested in [4].

Figure 3 (a) shows radial profiles of plasma parameters used as input data to simulate escaping neutral particle spectra in case of Maxwellian plasma ion distribution. Assumed Maxwellian proton energy PDF for two different $T_i(0)$ values is shown in Fig. 3 (b). Figure 3 (c) shows the resultant PDF for kinetic energies of H^0 atoms measured along the specified observation direction.

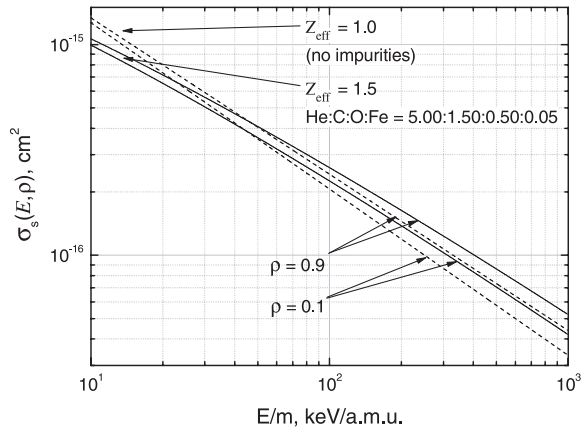

Fig. 2 Stopping cross section for neutral hydrogen in pure hydrogen plasma and in presence of impurities.

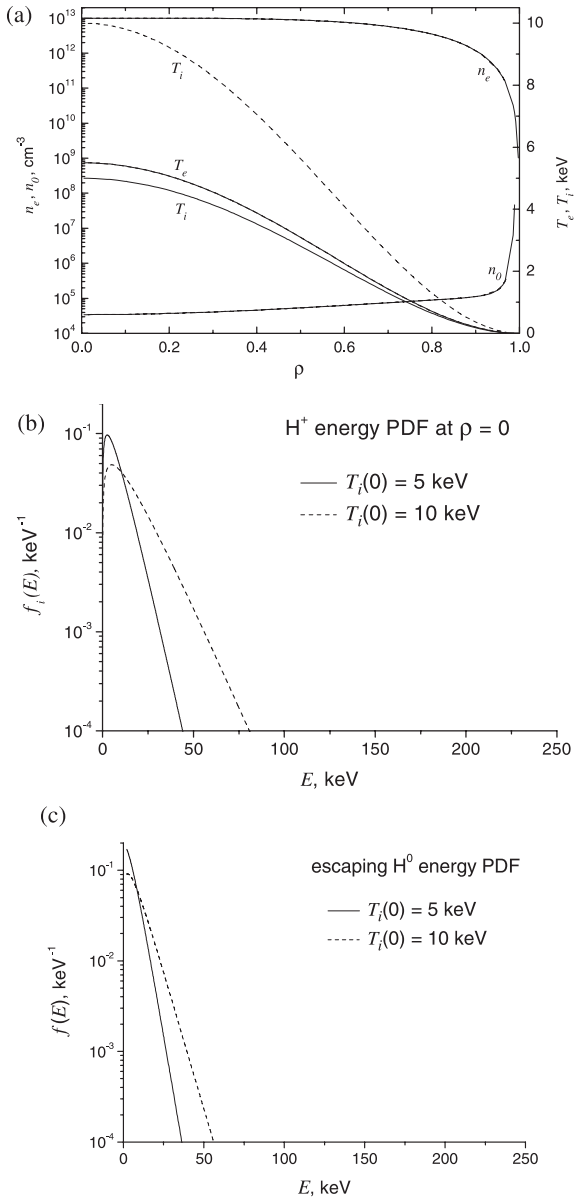

Fig. 3 (a) Input data for escaping H^0 energy distribution calculation in case of Maxwellian ion distribution for two different ion temperatures; (b) Maxwellian ion energy PDF in the plasma core for two temperatures; (c) calculated escaping H^0 energy PDF.

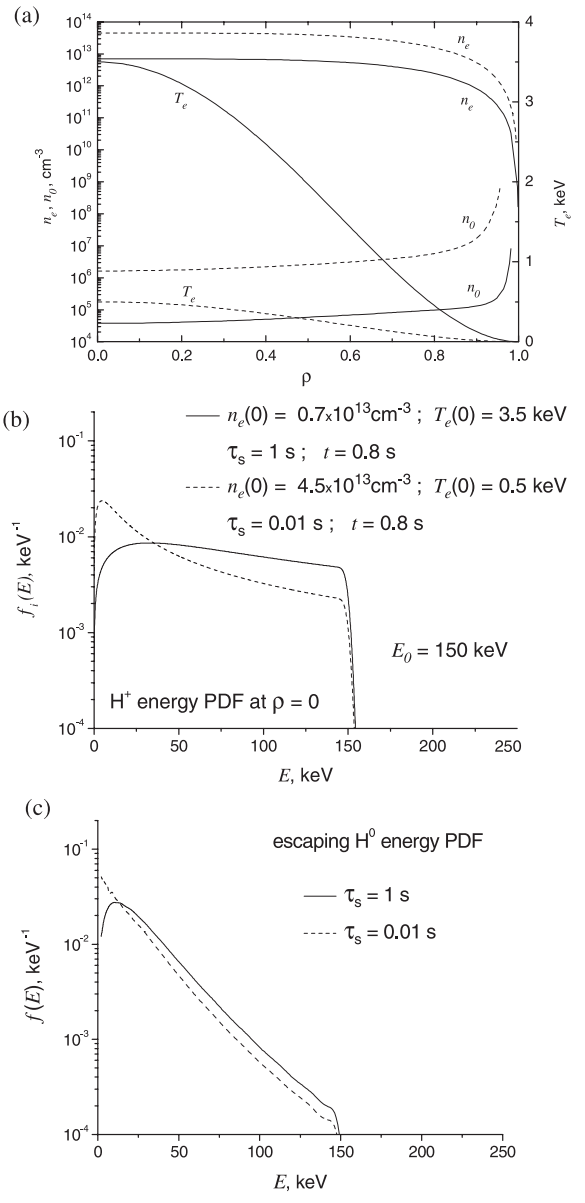

Fig. 4 (a) Input data for escaping H^0 energy distribution calculation in case of classical slowing down ion distribution for two different slowing down times; (b) ion energy PDF in the plasma core for two different slowing down times; (c) calculated escaping H^0 energy PDF.

Figure 4 (a) shows radial profiles of plasma parameters used as input data to simulate escaping neutral particle spectra in case of the classical slowing down distribution of plasma ions. Assumed proton energy PDF at $t = 0.8$ s is shown in Fig. 4 (b) for injection energy $E_0 = 150$ keV and two different pairs of the target plasma $n_e(0)$ and $T_e(0)$ values, i.e., for two different slowing down time values $\tau_s = 1$ s and $\tau_s = 0.01$ s. Figure 4 (c) shows the resultant PDF for kinetic energies of H^0 atoms measured along the specified observation direction in these two cases. Histograms of the corresponding pseudorandom number samples governed by these neutral particle energy PDFs are shown in Fig. 5 (a) for the Maxwellian case and in Fig. 6 (a) for the case of the classical slowing down distribution.

5. Data Processing Method

As an improvement of the neutral particle diagnostic data analysis, we have applied the probability density estimation using kernel smoothing techniques, e.g., [13, 14]. Given a sample of N random energy values, first consider the empirical PDF defined in [15]

$$f^{(e)}(E) = \frac{F^{(e)}(E+h) - F^{(e)}(E-h)}{2h}, \quad h > 0, \quad (19)$$

which is in fact the central difference derivative of the empirical CDF

$$F^{(e)}(E) = \frac{\#\{E_j : E_j \le E\}}{N}, \quad (20)$$

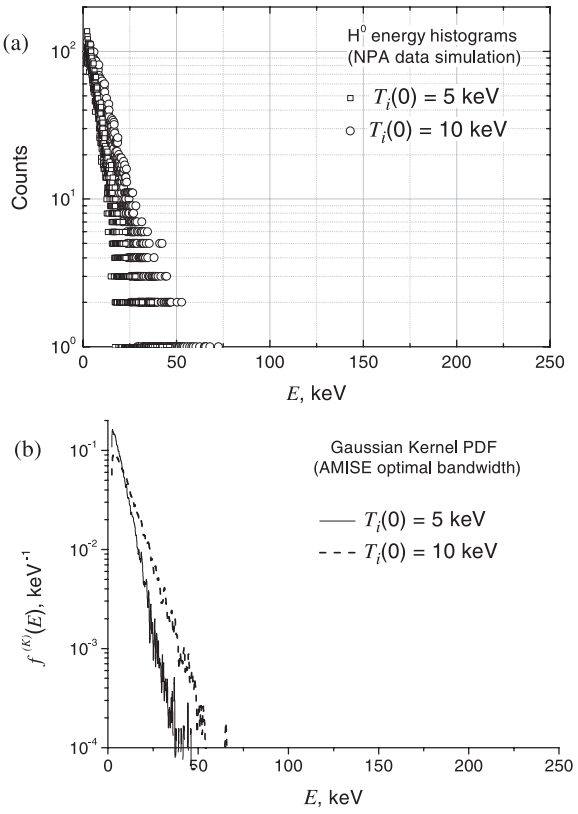

Fig. 5 (a) Histograms of pseudorandom numbers distributed as energies of escaping neutral atoms in case of Maxwellian ion distribution for two different ion temperatures; (b) Gaussian kernel PDF for H^0 energies calculated from the simulated random samples.

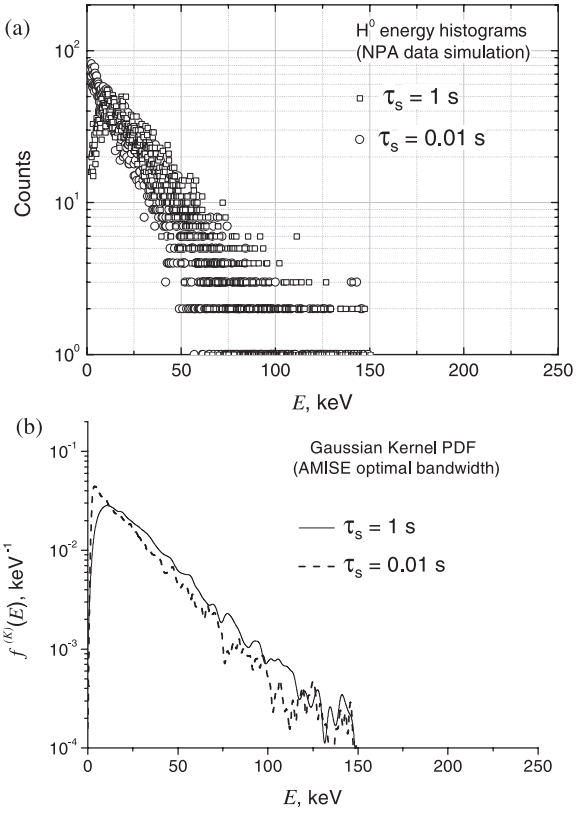

Fig. 6 (a) Histograms of pseudorandom numbers distributed as energies of escaping neutral atoms in case of classical slowing down ion distribution for two different slowing down times; (b) Gaussian kernel PDF for H^0 energies calculated from the simulated random samples.

also known as Kaplan-Meier cumulative distribution function. To describe its accuracy with respect to the unknown exact CDF $F(E)$, Kolmogorov statistic $D_N = \sup_E |F^{(e)}(E) - F(E)|$ and its tabulated asymptotic distribution $\lim_{N\to\infty} P(D_N \sqrt{N} \le y) = K(y),\ y > 0$ are used [16].

Next, consider a generalization of formula (19) called kernel PDF estimate, written as

$$f^{(K)}(E) = \frac{1}{Nh} \sum_{j=1}^{N} K\left(\frac{E - E_j}{h}\right), \quad h > 0, \tag{21}$$

which is determined by the kernel function $K(z)$ and the kernel bandwidth h. Formula (19) is a particular case of (21), when $K(z) = I_{(-1,1)}(z)$, and the rectangular function $I_{(-1,1)}(z)$ equals unity within $(-1, 1)$ interval and equals zero outside. The performance criterion of the kernel PDF estimation, also referred to as Parzen window method with respect to the unknown exact PDF $f(E)$, is the value of the mean integrated squared error

$$\mathrm{MISE}\left(f^{(K)}, f\right) = \left\langle \int_0^{+\infty} \left[f^{(K)}(E) - f(E)\right]^2 \mathrm{d}E \right\rangle, \tag{22}$$

where the averaging is performed over different samples of N realizations $(E_1, \ldots, E_N)$, and its "asymptote" for $N \gg 1$ (large sample approximation)

$$\mathrm{AMISE}\left(f^{(K)}, f\right) = \frac{c_1}{Nh} + \frac{c_2 c_3^2 h^4}{4}, \tag{23}$$

where $c_1 = \int K^2(z)\mathrm{d}z$, $c_2 = \int (f''(z))^2\,\mathrm{d}z$, and $c_3 = \int z^2 K(z)\mathrm{d}z$. The optimum kernel derived in [17] is Epanechnikov function $K(z) = \frac{3}{4}\left(1 - z^2\right) I_{(-1,1)}(z)$. However, it is emphasized [13,14] that the kernel function shape has a small influence on the method performance, while the bandwidth parameter h is more important. Therefore, Gaussian kernel

$$K(z) = \frac{1}{\sqrt{2\pi}} e^{-z^2/2} \tag{24}$$

has been used, since it has a continuous derivative.

A reliable practical method for optimum h selection was proposed in [18] and revisited recently in [19]. The bandwidth is obtained by solving the equation

$$h = \left(\frac{1}{2\sqrt{\pi} N \phi_4(\eta(h))}\right)^{1/5}, \tag{25}$$

where the function ϕ_r is expressed via kernel derivative

$$K^{(r)}(z) = (-1)^r He_r(z) K(z) \tag{26}$$

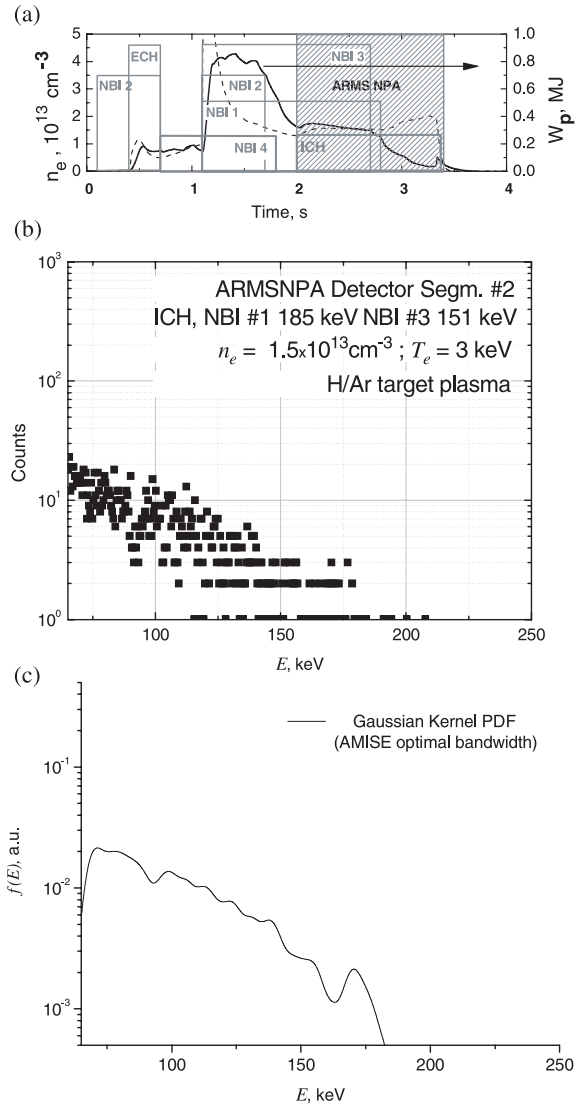

Fig. 7 (a) Background plasma parameters and ECH/ICH/NBI heating time diagram; (b) experimental histogram of escaping H^0 energies measured by ARMS NPA along sight line #2; (c) calculated H^0 energy PDF with Gaussian kernel and AMISE-optimal smoothing parameter.

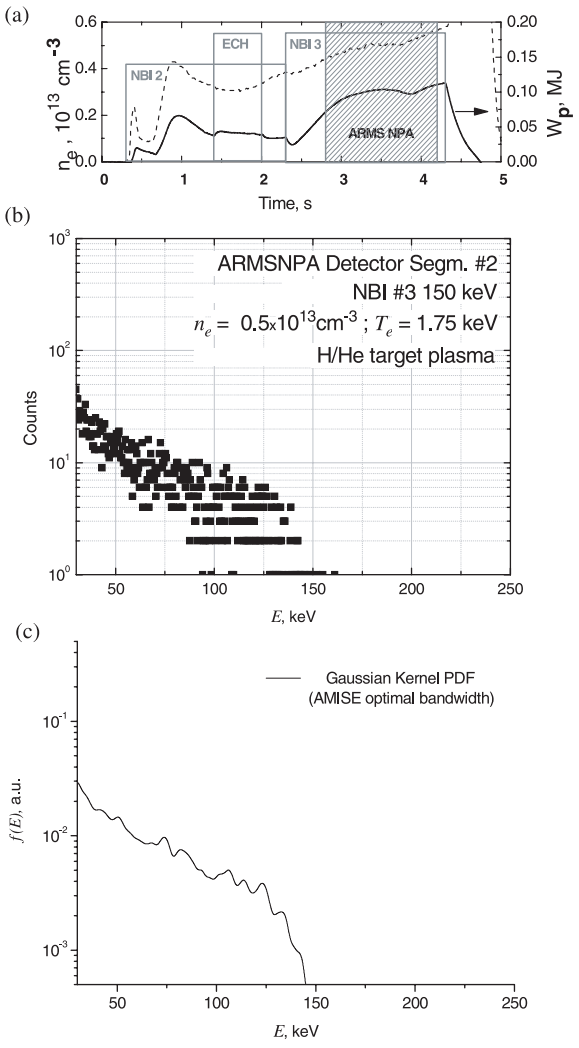

Fig. 8 (a) Background plasma parameters and ECH/NBI heating time diagram; (b) experimental histogram of escaping H^0 energies measured by ARMS NPA along sight line #2; (c) calculated H^0 energy PDF with Gaussian kernel and AMISE-optimal smoothing parameter.

as follows

$$\phi_r(h) = \frac{1}{N(N-1)h^{(r+1)}} \sum_{i=1}^{N} \sum_{j=1}^{N} K^{(r)}\left(\frac{E_i - E_j}{h}\right). \tag{27}$$

$He_r(z)$ designates rth degree modified Hermite polynomial [20]. The function

$$\eta(h) = \left(\frac{-6\sqrt{2}\phi_4(a)}{\phi_6(b)}\right)^{1/7} h^{5/7} \tag{28}$$

depends on the values

$$a = \left(\frac{16\sqrt{2}}{5N}\right)^{1/7} \hat{\sigma} \quad \text{and} \quad b = \left(\frac{480\sqrt{2}}{105N}\right)^{1/9} \hat{\sigma}, \tag{29}$$

where

$$\hat{\sigma} = \sqrt{\frac{1}{N-1}\sum_{i=1}^{N}\left(E_i - \bar{E}\right)^2}, \quad \text{and} \quad \bar{E} = \frac{1}{N}\sum_{i=1}^{N} E_i. \tag{30}$$

Direct implementation of formula (27) is slow. An approximate fast calculation technique to the required precision is given in [19].

These methods have been tested by constructing the kernel probability density function from the generated pseudorandom number samples assuming Maxwellian ion energy distribution shapes for different temperatures and classical slowing down distributions with different slowing down times. The test results of these numerical experiments are shown in Figs. 5 (b) and 6 (b).

Application of the methods described above to the analysis of passive chord-integrated experimental data obtained with the Angular-Resolved Multi-Sightline Neutral

Particle Analyzer on Large Helical Device is illustrated in Figs. 7 and 8. Figures 7 (a) and 8 (a) summarize the experimental conditions and heating time diagrams for H/Ar target plasma heated by ICH and parallel NBI and for H/He target plasma heated by parallel NBI alone. The experimental setup is explained in detail in [2, 21]. Experimentally obtained histograms of fast neutral particles measured by ARMS NPA chord #2 during the shaded time intervals are shown in Figs. 7 (b) and 8 (b). These histograms were automatically calculated by Clear Pulse Model 1219 CAMAC PHA module used for digital processing of detector signals formed by a resistive feedback charge sensitive preamplifier and a shaping amplifier [2].

Figures 7 (c) and 8 (c) illustrate the probability density functions for energetic neutral particles from suprathermal distribution tails above 70 and 30 keV, respectively, obtained by Gaussian kernel smoothing (21) with AMISE optimal bandwidth parameter calculated using (25)-(30).

It should be noted that the obtained $f^{(K)}(E)$ is a normalized, smooth continuous function, which is an approximation to the unknown true PDF for neutral particle energies. The approximation criterion is the minimization of AMISE (23) by choosing the kernel bandwidth parameter. This approximation is based on the experimentally obtained random sample of escaped particle energies measured using a solid state detector in combination with a charge sensitive amplifier and an optional pulse shaping amplifier. Thus, the method inherits the energy resolution properties of the pulse processing electronic circuit. Digital processing of charge sensitive amplifier output signal might be preferable.

6. Summary

The goal of neutral particle diagnostics is to obtain information about the ion distribution function and especially its substantially non-Maxwellian high energy "tail." This is important for ion heating and confinement studies. Such measurements are not direct. The relationship between the ion distribution function and the probability density for escaping charge-exchange neutral particle kinetic energies has been derived in a general form for chord-integral passive measurements from a magnetic confinement fusion plasma column. A calculation method has been realized that has a predictive force to simulate the experimentally measurable random samples of escaping neutral atom energies for any given plasma ion distribution, electron density and temperature profiles, plasma composition, and experimental geometry. This is a "direct calculation" to obtain random escaping atom energy sample from the known plasma ion distribution. A method to solve the "inverse problem" has also been proposed, which is based on Gaussian kernel smoothing with automatic choice of AMISE-optimal bandwidth parameter. Thus, neutral atom energy probability density function is obtained from the experimental random samples. This PDF for escaped neutral atom energies can then be used to study the ion distribution function within the plasma. The proposed method is applicable for diagnostics based on solid state detectors. "Raw" data obtained directly from PHA ADC is required to obtain samples of particle energies rather than the less informative, automatically built histogram PDF estimators.

Acknowledgment

This work was supported by Grant-in-Aid for JSPS Fellows No. 1806173.

[1] P.R. Goncharov, J.F. Lyon, T. Ozaki *et al.*, J. Plasma Fusion Res. SERIES **5**, 159 (2002).
[2] E.A. Veshchev, T. Ozaki, P.R. Goncharov *et al.*, Rev. Sci. Instrum. **77**, 10F129 (2006).
[3] P.R. Goncharov, T. Ozaki and S. Sudo, Proc. 34th EPS Conf. Plasma Phys. P5.081 (2007).
[4] R.K. Janev, C.D. Boley and D.E. Post, Nucl. Fusion **29**, 2125 (1989).
[5] J.G. Cordey and M.J. Houghton, Nucl. Fusion **13**, 215 (1973).
[6] M. Matsumoto and T. Nishimura, ACM Trans. Model. Comput. Simul. **8**, 3 (1998).
[7] S.P. Hirshman and J.C. Whitson, Phys. Fluids **26**, 3553 (1983).
[8] Yu.N. Dnestrovskij *et al.*, Nucl.Fusion **19**, 293 (1979).
[9] Yu.S. Gordeev *et al.*, JETP Lett. **25**, 204 (1977).
[10] R.K. Janev, W.D. Langer *et al.*, *Elementary Processes in Hydrogen-Helium Plasmas* (Springer-Verlag, Berlin, 1987).
[11] C.F. Barnett, ed., *Atomic Data for Fusion*, ORNL-6086 vol. **1** (Controlled Fusion Atomic Data Center, Oak Ridge, TN, 1990).
[12] H. Hughes, D.E. Post, Journ. Comput. Phys. **28**, 43 (1978).
[13] A.W. Bowman and A. Azzalini, *Applied smoothing techniques for data analysis* (Clarendon, 1997).
[14] M.P. Wand and M.C. Jones, *Kernel Smoothing* (Chapman and Hall, London, 1995).
[15] M.S. Waterman and D.E. Whiteman, Int. J. Math. Educ. Sci. Technol. **9**, 127 (1978).
[16] L.N. Bolshev and N.V. Smirnov, *Tables of mathematical statistics* (Nauka, Moscow, 1983).
[17] V.A. Epanechnikov, Theory Probab. Appl. **14**, 153 (1969).
[18] S.J. Sheather and M.C. Jones, J.R. Statist. Soc. B **53**, 683 (1991).
[19] V.C. Raykar and R. Duraiswami, *Very fast optimal bandwidth selection for univariate kernel density estimation* (University of Maryland, CS-TR-4774/UMIACS-TR-2005-73, 2006).
[20] M. Abramowitz and I.A. Stegun, eds., *Handbook of mathematical functions* (Dover, New York, 1972).
[21] E.A. Veshchev, T. Ozaki, P.R. Goncharov *et al.*, Plasma Fusion Res. **2**, S1073 (2007).